

# Intelligent control and performance evaluation of a novel precise positioning stage

Guang-Qing Lu<sup>a,\*</sup>, Audrius Čereška<sup>b</sup>, Giedrius Augustinavičius<sup>b</sup>, Rimas Maskeliunas<sup>b</sup> and Minvydas Ragulskis<sup>c</sup>

<sup>a</sup>*School of Electrical and Information Engineering, Jinan University, Zhuhai, China*

<sup>b</sup>*Department of Mechanical Engineering, Vilnius Gediminas Technical University, Vilnius, Lithuania*

<sup>c</sup>*Department of Mathematical Modelling, Kaunas University of Technology, Kaunas, Lithuania*

**Abstract.** A novel planar precise positioning stage on the rotating platform for calibration on raster scales of the rotary encoder is proposed in this paper. The monolithic structure is constructed with a flexible element and two ultra-fine adjustment screws. The structure for required motion is designed and optimized by software package of Solid Works Simulation, and then their performances are evaluated using numerical modelling approach. The mathematical model is then verified by resorting to finite element analysis (FEA) and experiment. The established analytical FEA models are helpful for optimizing a reliable architecture and improving performance of the precise positioning system.

Keywords: Positioning stage, flexible element, finite element analysis, simulation

## 1. Introduction

Many modern micro positioning systems operate with the conventional techniques that compose stepper, servomotors, micro hydraulic or pneumatic actuators. In such systems, main reciprocating or rotary motion transmission mechanisms are bearings, which have such shortcomings as friction, wear, idling and assembly errors, etc., and thus need lubrication. One way to increase the positioning accuracy is application of solid flexible mechanisms.

Precise flexible mechanisms are very widely applied in micro/nano-positioning a plane [1] and or three dimensional positioning. They are also used for various devices in optics, telecommunications, photo and laser industries. Where, it is necessary to obtain

the output resolution in micrometer or nanometer for the platform displacement.

The simplest mechanism is a single composite flexible connector. Many micro positioning systems are developed by use of solid and flexible mechanisms for positioning one axis [2–4].

Combining two positioning systems into a single structure increases greatly the geometric parameters of a positioning system. Positioning system in literatures [5, 6] was operated with one piezo gauge in directions of x- and y-axes, and the positioning system containing two piezo gauges in literatures [7–9] controlled its x- and y-directions.

Researchers investigated the scheme for revolutionary positioning systems with three degree of freedoms (DOFs) in space, which may move along the directions of x-, y- and z-axes [10–12]. Micro positioning systems with three rotational DOFs were designed with flexible connectors, composing of three piezo gauges, thus increasing the product cost, and positioning in x- and y-directions, situating on

the  $120^\circ$  actuators. But they were still complicated [13, 14].

The design and modeling of 3-DOF flexure-based parallel [15–17] and pyramidal-shaped piezo-driven mechanisms [18, 19] were also introduced, respectively. For instance, Yung et. al presented the model reference adaptive control for a piezo-positioning system [20].

The mechanism of the deformed joints with one axis, and or with symmetrical, circumferential and multiple axes was studied, respectively [21, 22], where six piezo gauges were used in the mechanism, of which the proceeding was  $13\ \mu\text{m}$ . It was divided into three deformable groups set every  $120^\circ$ . Deformable flexible stiffness matrix was formulated using second Castigliano's theorem. Input and output dependence shifts were also presented in the researches.

The input link analysis method of three revolutions to deform mechanism was given by Wang et al. [23]. The results obtained from the numerical method were verified by finite element analysis (FEA) via software package ANSYS, and by experiments.

Mechanism designed and sandwiched by means of deformable bridge-type shear strengthening was presented with some results in literature [24]. It produced the output displacement in vertical direction of operating input displacement. The stiffness of this type of mechanisms is thus much higher than that of ordinary deformable mechanisms with deformable bridge. Such a mechanism is relatively compact and results in relatively high gear ratio, as well as the stiffness, in comparison to a simple bridge type of enhancement. It has been drawn up mathematical model to set the gear ratio, using Euler-Bernoulli theory. Its bridge-type shear compliance was simulated in literature [25] with optimized results.

Literatures [26–28] provided the positioning system in x- and y-directions, combining the parallel mechanisms with four twin-type bridges and four deformable beams into a single structure. The system was designed with high ratio 3.09 and proceedings  $290 \times 290\ \mu\text{m}$ , but the deviations of moving trajectories from straight linearity in directions of positioning axes could be even up to 6.2%.

A deformable mechanism with three twists was developed by use of kinetic and dynamic analysis [29]. The operating upper-limits of the nano-positioning system were  $27\ \mu\text{m}$  and  $18\ \mu\text{m}$  at x- and y-coordinates, respectively, and all three actuators could be rotated  $1.72^\circ$  with systematic natural frequency at 463 Hz.

Mechanism with spherical deformable bridge was also studied and presented [30]. It consists of two bridges connected in horizontal and vertical directions. Displacement errors could be eliminated, because the bridges were connected rigidly.

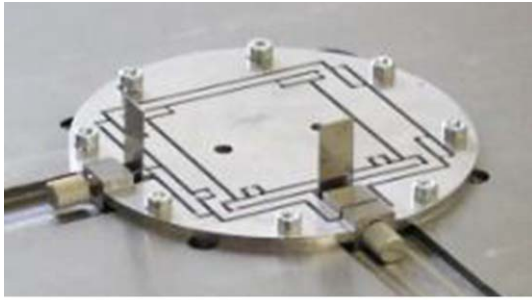
Yong, et al. [31] investigated how to change the accuracy characteristics of a deformable hinge, including its radius R, joint thickness T and their ratio T/R. The equations determining the stiffness were used for 3RRR precise positioning systems, such as Paros (full), Paros (simplified), Lobontiu, Wu, Tseytlin, Smith and Schotborgh. The dependence on R and T could be provided by the equations. The kineto-static model of 3RRR deformable mechanism was established as well [32]. Moving trajectory deviations of micro positioning systems from rectilinear course can be obtained by conventional technical approach, resulting in  $100\ \mu\text{m}$ , greater than  $2\ \mu\text{m}$ .

Modern technologies evolve rapidly and increase the demand of micro positioning systems, capable of positioning with higher accuracy, operating over a wider range, and ensuring reduction on moving trajectory deviations from rectilinear course but with smaller geometric parameters simultaneously. Some literatures demonstrate that a large number of micro positioning systems are operating based on principle of prospective continuous flexible mechanisms. Nevertheless, the existing micro positioning systems with two axles created through flexible connector are still difficult for positioning the raster and code scales, and if designed improperly, both geometrical parameters and weight would be excessive and thus reduce the accuracy. Therefore, a new positioning system is needed to be developed to improve the current systems further.

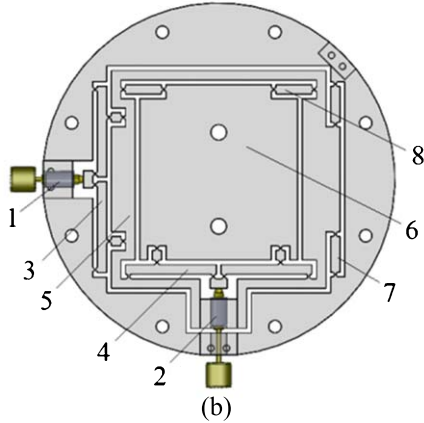
In this study, a new designed precise positioning mechanism system is proposed to ensure high positioning accuracies in directions of x- and y-axes simultaneously. In addition, analytical results for the system are provided, together with relevant FEA simulation and experimental measurement.

## **2. Installing Construction scheme and working principle**

A dual axis flexure-based micro positioning stage on the rotating platform for calibrating the raster scales of rotary encoder is theoretically modeled here. The stage is used to achieve the motion in a desired direction. For a linear stage, the motion is along an ideal straight line, therefore, any motion in a



(a)



(b)

Fig. 1. Dual axis micro positioning stage with mechanical actuation: (a) micro positioning stage (photo); (b) top view of the stage (transparent): 1, 2 – super-fine adjustment screws, 3, 4 – motion reduction mechanisms, 5 –  $x$ -axis moving platform, 6 –  $y$ -axis moving platform, 7, 8 – support mechanisms.

constrained direction will contribute to the deviation from ideal trajectory. A dual axis flexure-based micro positioning stage consists of a monolithic structure and two manual adjusters, similar to micrometres, to provide the motion, as shown in Fig. 1.

In Fig. 1, the high precise adjusters 1 and 2 avoid the complexity associated with the installations of hydraulic and pneumatic actuators and or the power supply. The adjustment screws are compact and provide extremely high resolution, including smooth and repeatable action via mating a high precision at  $200\ \mu\text{m}$  pitch. The handy dimensions of the knobs are optimally chosen to detect the rotation less to  $0.5^\circ$ – $1^\circ$  that enables to obtain the positioning sensitivity of  $0.5\ \mu\text{m}$ .

Adjustment screws are mounted into the monolithic structure rigidly. Both  $x$ - and  $y$ -axis moving platforms consist of input motion reduction mechanisms –3 and 5, and support mechanisms guiding the motion –7 and 8. The  $y$ -axis platform 6 has the same structure except that it is inside the  $x$ -axis platform 5. The motions in directions of  $x$ - and  $y$ -axes

are decoupled. Generally, a decoupled stage implies that one adjuster produces only one directional output motion without affecting the motions in the directions of other axes. The main target of the stage design is to eliminate the cross-axial coupling errors between the motions in  $x$ - and  $y$ -directions and parasitic rotation errors around the axes. The mechanism structure with symmetric lever reduces about three times of the input transfer ratio, and thus the straightness deviation. Therefore, the stage can be robust to temperature variation.

### 3. Analytical model

A monolithic compliant mechanism consists of flexure hinges and rigid links. The flexure hinge is a thin element, which allows the relative rotation between two rigid links and prohibits any other motions. Circular flexure hinge with single axis is chosen for its simple technical process, and has better accuracy characteristics, comparing with other types of flexure hinges, for its functionality – positioning in plane. It has the highest accuracy because the bending point is located at the centre of the hinge.

Although all the flexure hinges mentioned have many advantages, they have such disadvantages that the hinges are difficult to be described mathematically. Additionally, the end of a free flexure hinge has six DOFs, three translational and three rotational. The bending centre of a circular flexure hinge with single axis rotates about the hinge centre and translates in the directions of  $x$ - and  $y$ -axis. Therefore, replacing each flexure hinge by an elastic element with different coefficients of stiffness and damping, and assuming that the other elements are rigid bodies, the analytical dynamic model of a micro positioning stage can be established consequently.

The sensitivity of a positioning mechanism to vibration depends on its natural frequencies. The flexure-based micro positioning stage can be considered as a ‘spring–mass’ system, subsequently, characterizing its general dynamic behaviour is important.

On the basis of multibody dynamics, each the flexure hinge can be replaced by a rotational and translational joint with a linear and torsion spring, while the rest elements are considered as rigid bodies. Then, the dynamic model of a micro positioning stage with dual axis can be well established. There are generally two translations in  $x$ - and  $y$ -directions and one rotation,  $\varphi$ , about the sensitive axis of the hinge.

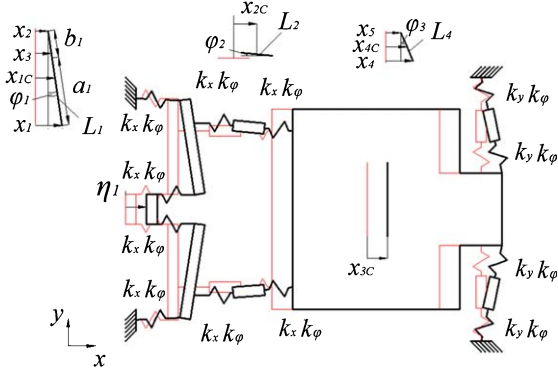


Fig. 2. Dynamic model of precise positioning stage forced by virtual input displacement.

The dynamic analysis on flexure-based mechanisms can be carried out by means of Lagrange's equations based on scalar quantities of kinetic, potential and dissipative energies.

Vibrations on the stage are generally small. Thus, the stage location in dynamic model can be defined by Descartes coordinate system in  $xOy$ -plane. In statics, initial point  $O$  at the coordinate system matches with the point at where force  $F_x$  is applied to the stage. The micro positioning stage is excited by virtual input displacement  $\eta_1$  along the symmetric axis dividing the stage. Therefore, motion along  $y$ -axis is impossible theoretically, as shown in Fig. 2. The virtual translational and rotational displacements are defined by generalized coordinates  $(x_1, x_{2C}, x_5, x_{3C}, \varphi_1, \varphi_3)$  and auxiliary coordinates  $(x_2, x_{1C}, x_3, x_4, x_{4C})$  expressed by the generalized coordinates.

The dynamic model of the precise positioning stage is shown in Fig. 2. The important design properties for any type of flexure hinge include the stiffness in rotational direction  $z$ , the stiffness in  $x$ - and  $y$ -directions and the stress built by bending or elastic deformation over an angle  $\varphi$ .

Aluminium alloy (AL7075-T6) and steel are often used as base materials for flexure hinges. In this analysis, the former one is selected to be the material due to its excellent phase stability and high strength.

Ultimately, the geometric parameters of the flexure hinges and rigid links in the mechanism system are fixed in consideration of maximum stresses under bending.

The workspace of a dual axis flexure-based micro positioning stage depends primarily on the moving range permitted by the elastic range of the flexure hinges and the input displacement. Thus, its analysis can be dealt completely in terms of the constraints due

to the allowable rotational and translational ranges on the hinges. A schematic of the hinge being used is shown in Fig. 2c, for which the equations of Paros [33] are used to calculate its angular compliance:

$$K_\varphi = \frac{\Delta\varphi_z}{M_z} = \frac{24r}{Ewt^3(2r+t)(4r+t)^3} \left( t(4r+t)(6r^2+4rt+t^2) + 6r(2r+t)^2\sqrt{t(4r+t)}\tan^{-1}\sqrt{1+\frac{4r}{t}} \right) \quad (1)$$

Then, the rotational stiffness of circular flexure hinge is:

$$k_\varphi = \frac{1}{K_\varphi} \quad (2)$$

And the translational compliance in direction of  $x$ -axis is:

$$K_x = \frac{\Delta x}{F_x} = \frac{1}{Eh} \left[ \frac{2(2r+t)}{\sqrt{t(4r+t)}} \tan^{-1} \left( \sqrt{1+\frac{4r}{t}} - \frac{\pi}{2} \right) \right] \quad (3)$$

Thus the translational stiffness of the circular flexure hinge in direction of  $x$ -axis is:

$$k_x = \frac{1}{K_x} \quad (4)$$

And the translational compliance in direction of  $y$ -axis can be obtained as:

$$K_y = \frac{\Delta y}{F_y} = \frac{3}{4Ewt(2r+t)} \left( \frac{2r(2+\pi) + \pi t + \frac{8r^3(44r^2+28rt+5t^2)}{(4r+t)^2 t^2} + \frac{1}{\sqrt{t^5(4r+t)^5}}}{\left( (2r+t)\sqrt{t(4r+t)}[24tr^3 + (\pi-80)r^4 + 8(3+2\pi)r^2 t^2 + 4(1+2\pi)t^3 r] + t^2 - 16r(2t-3r)(2r+t)^4 \right)} \right) \tan^{-1} \sqrt{1+\frac{4r}{t}} \quad (5)$$

The translational stiffness in direction of  $y$ -axis is then:

$$k_y = \frac{1}{K_y} \quad (6)$$

Where,  $t$ ,  $r$ ,  $w$  and  $h$  – thickness, radius, width, and height of the flexure hinge;  $E$  – Young's Modulus of hinge material;  $\Delta\varphi$  – angular deformation of the hinge about  $z$ -axis in radian;  $M$  – external bending torque applied to the hinge, which can be probably

used to determine the allowable rotational range;  $\Delta x$ ,  $\Delta y$  – linear deformations of the hinge in directions of  $x$ - and  $y$ -axes;  $F_x$ ,  $F_y$  – external translational forces applied to the hinge in directions of  $x$ - and  $y$ -axes.

Because the motions of the stage in directions of  $x$ - and  $y$ -axes are decoupled, it can be assumed that, the motion in direction of  $x$ -axis is the same as that in direction of  $y$ -axis. For this reason, only the motion along a single axis is analyzed further. The micro positioning stage with single axis consists of twelve elastic elements, including flexure hinges designed with identical dimensions, and eighth rigid bodies, as shown in Fig. 2. They follow the following equation:

$$\frac{d}{dt} \left( \frac{\partial T}{\partial \dot{q}_i} \right) - \frac{\partial T}{\partial q_i} + \frac{\partial \Phi}{\partial \dot{q}_i} + \frac{\partial \Pi}{\partial q_i} = F_i(t) \quad (7)$$

$(i = 1, 2, \dots, n)$

Where,  $T$  – kinetic energy;  $\Pi$  – potential energy;  $\Phi$  – dissipative energy;  $q_i$  – the  $i$ -th generalized Lagrangian coordinate at generalized coordinate  $(x_i, \varphi_i)$ ;  $F_i$  – generalized force in direction of coordinate  $q_i$ .

The kinetic energy of the micro positioning stage can be consequently expressed by:

$$T = m_1(\dot{x}_2 + L_1\dot{\varphi}_1)^2 + I_{1C}\dot{\varphi}_1^2 + m_2\dot{x}_{2C}^2 + \frac{1}{2}m_3\dot{x}_{3C}^2 + m_4 \left( \dot{x}_5 + \frac{L_4}{2}\dot{\varphi}_3 \right)^2 + I_{4C}\dot{\varphi}_3^2 \quad (8)$$

And the potential energy of the stage can be expressed as:

$$\begin{aligned} \Pi = & k_x(x_2 + L_1\varphi_1 - \eta_1)_i^2 + 3k_\varphi\varphi_1^2 \\ & + k_x x_2^2 + k_x(x_{2C} - x_2 + b_1\varphi_1)^2 \\ & + k_x(x_{3C} - x_{2C})^2 + 2k_\varphi\varphi_3^2 + \\ & k_y(x_5 + L_4\varphi_3 - x_{3C})^2 + k_y x_5^2 \end{aligned} \quad (9)$$

Correspondingly, the dissipative energy of the stage can be determined by:

$$\begin{aligned} \Phi = & c_x(\dot{x}_2 + L_1\dot{\varphi}_1 - \dot{\eta}_1)_i^2 + 3c_\varphi\dot{\varphi}_1^2 + \\ & c_x\dot{x}_2^2 + c_x(\dot{x}_{2C} - \dot{x}_2 + b_1\dot{\varphi}_1)^2 + \\ & c_x(\dot{x}_{3C} - \dot{x}_{2C})^2 + 2c_\varphi\dot{\varphi}_3^2 + c_y(\dot{x}_5 \\ & + L_4\dot{\varphi}_3 - \dot{x}_{3C})^2 + c_y\dot{x}_5^2 \end{aligned} \quad (10)$$

Where,  $\eta_1$  – input displacement;  $k_x$ ,  $k_y$ ,  $k_\varphi$  – stiffness coefficients;  $c_x$ ,  $c_y$ ,  $c_\varphi$  – viscous damping coefficients,  $L_1$ ,  $L_4$ ,  $b_1$  – geometrical parameters of the compliant mechanism.

Since solving these equations is time consuming, it is programmed using software package of MATLAB/Simulink to (i) form analytical expressions of

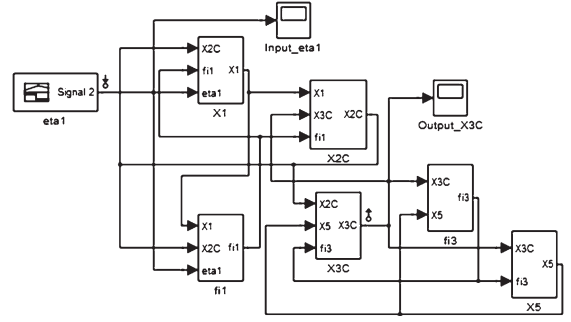


Fig. 3. Simulink model of the micro positioning stage.

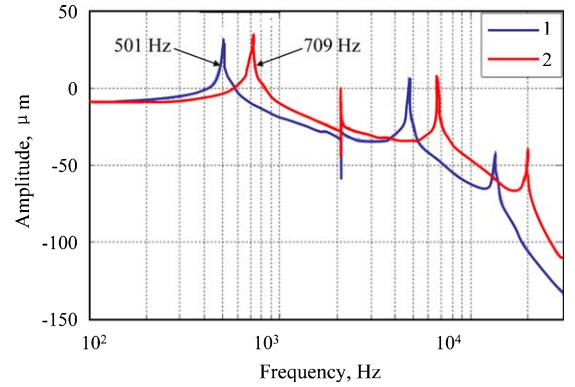


Fig. 4. Resonant frequency of the micro positioning stage: 1 – along  $x$ -axis, 2 – along  $y$ -axis.

the kinetic, potential and dissipative energies, (ii) differentiate them with respect to generalized coordinates  $x_i$ ,  $\varphi_i$  and time  $t$ , (iii) transform them into the form of operator, (iv) solve the established differential equation system with respect to generalized coordinates  $x_i$  and  $\varphi_i$ , and (v) generate the matrices with all the data required to construct the architectural diagram and Simulink-model for the micro positioning stage, as shown in Fig. 3. Final Simulink model contains a number of subsystems. Where, two oscilloscopes are integrated into the Simulink model for monitoring the signals of input and output displacements.

The natural frequencies of corresponding dynamic model are 501 Hz and 709 Hz in directions of  $x$ - and  $y$ -axes, respectively, as shown in Fig. 4. Note that the vibration of the device is considered according to the schematic diagram presented in Fig. 2 and the corresponding discrete model described by Equations 7–10.

In case of the input displacement of 350  $\mu\text{m}$  applied to the stage, the analytical model provides

that, the output platform translates by displacement of  $116.5\ \mu\text{m}$  and the maximum stress occurs at  $454.5\text{MN}/\text{m}^2$ , which is 90% of the yield strength of aluminium alloy AL7075-T6. When the smallest input displacement of  $0.5\ \mu\text{m}$  is applied, the output platform translates by displacement of  $0.162\ \mu\text{m}$ . Moreover, the analytical results show that the reduction ratio of the precise positioning stage is about  $0.330\ \mu\text{m}$ .

#### 4. Model verification by FEA

To verify the analytical model, finite element analysis (FEA) on the targeted precise positioning stage is performed by software package ANSYS. The principal designed factors of the hinge mechanism are structural geometries and material properties. Material elastic deformation is primarily taken into account for the mechanism. If hinge deformation is over the elastic limit, plastic deformation occurs and the hinge lifetime is shortened significantly.

The following invariable boundary conditions are assumed in FEA simulation:

- 1) The super-fine adjustment screws are rigid bodies, therefore their deformations won't be taken into account;
- 2) The holes on the stage are fixed rigidly;
- 3) Aluminium alloy AL7075-T6 is chosen to construct the monolithic structure due to its properties: small elastic modulus  $7.20 \times 10^{10}\ \text{N}/\text{m}^2$  and high yield strength  $5.03 \times 10^8\ \text{N}/\text{m}^2$ ;
- 4) All parts are bonded with no clearance;
- 5) The gravity force is applied vertically at the gravitational acceleration of  $9.81\ \text{N}/\text{m}^2$ .

Two testing steps for FEM analysis on the stage are implemented:

**Step 1.** The maximum input displacement until elastic limit of deformation is simulated firstly;

**Step 2.** The minimum adjustable input displacement is then simulated.

In Step 1, when input displacement of  $350\ \mu\text{m}$  is applied in direction of  $x$ -axis, it can be obtained that, the output platform translates by displacement of  $111.53\ \mu\text{m}$ , as shown in Fig. 5a), and the maximum stress occurs at  $464.3\ \text{MN}/\text{m}^2$ , which is 91.9% of the yield strength of the alloy AL7075-T6; When input displacement of  $350\ \mu\text{m}$  is applied in direction of  $y$ -axis, the output platform translates by displacement of  $113.05\ \mu\text{m}$ , as shown in Fig. 5b), and the maximum stress occurs at  $465.8\ \text{MN}/\text{m}^2$ , which is 92.2%

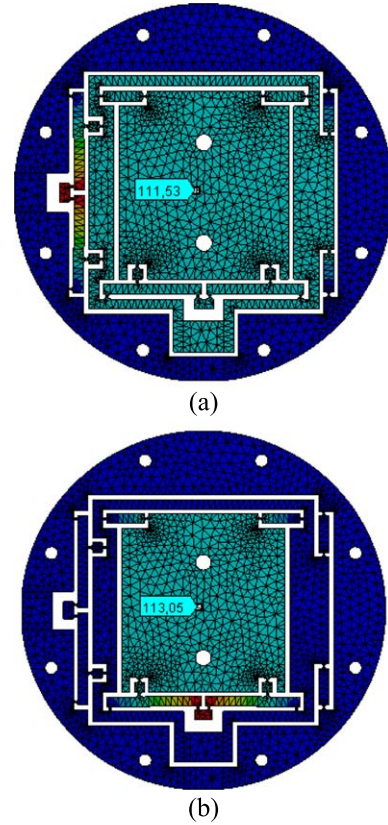


Fig. 5. FEM model of the precise positioning stage: (a) input displacement of  $350\ \mu\text{m}$  applied in  $x$ -direction; (b) input displacement of  $350\ \mu\text{m}$  applied in  $y$ -direction.

of the yield strength of the alloy AL7075-T6. Moreover, FEA results show also that the reduction ratio of the stage is about 0.308 in directions of  $x$ - and  $y$ -axes.

In Step 2, when the minimum input displacement of  $0.5\ \mu\text{m}$  is applied in direction of  $x$ -axis, the output platform translates by displacement of  $0.155\ \mu\text{m}$ ; When the minimum input displacement of  $0.5\ \mu\text{m}$  is applied in direction of  $y$ -axis, the output platform translates by displacement of  $0.157\ \mu\text{m}$ , as shown in Fig. 5. It is clear that nonholonomic and frictional interaction would have a major impact to the vibration of the FEA model of the device – however these interactions can be ignored if only static displacements of the table are considered.

#### 5. Experimental setup

For further validation, a flexure-based monolithic structure is designed and machined firstly using electro-discharge machining (EDM) technique to

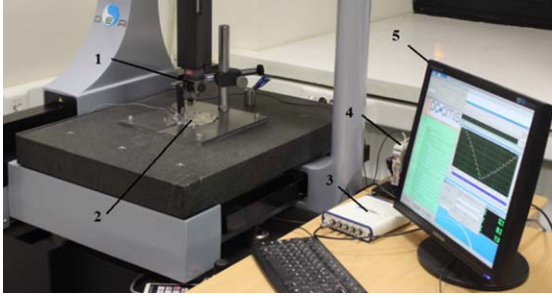


Fig. 6. Experimental setup of micro positioning stage: 1–touch trigger probe, 2–precise positioning stage, 3–dynamical signal analyser, 4–eddy current proximity sensor, 5–computer.

ensure the machining precision for the stage. In general, the hinge thickness is small and EDM process gives good repeatability and accuracy in order of 25–125  $\mu\text{m}$ . The achievable tolerances are  $\pm 2.5 \mu\text{m}$ . The surface finishness produced by EDM is usually in the range of 0.8–3.0  $\mu\text{m}$ , depending upon the machining conditions involved.

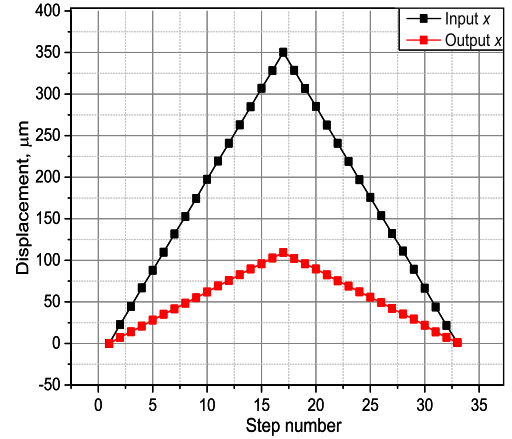
Then, two mechanical super-fine adjustment screws (S-867, Standa) are attached into the monolithic structure rigidly. Applying special screw design provides smooth and repeatable actions so that mate a high precision 200  $\mu\text{m}$  pitch and positioning resolution of 0.5  $\mu\text{m}$ . The finished experimental setup of a micro positioning stage is shown in Fig. 6.

The experimental micro positioning stage is fixed on Coordinate Measurement Machine (CMM, DEA Micro Hite, Hexagon Metrology). The input displacement of the stage is then measured by Eddy Current Proximity Sensor (ECPS, ECL202, Lion Precision) with measurement range of 500  $\mu\text{m}$  and a resolution of 30 nm on the CMM. Testing data from ECPS is processed by dynamical signal analyser (NI-USB-4432, National Instruments) and data acquisition (DAQ) system with high-performance and high-dynamic range.

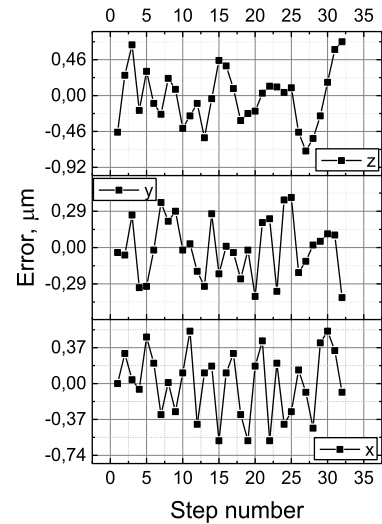
## 6. Results and discussions

For the experimental precise positioning stage, the simulated and predicted results at  $x$ - and  $y$ -positions versus input value  $\eta_1$  over the range of 350  $\mu\text{m}$  are plotted in Figs. 7(a) and 8(a), respectively. The experiment shows that, within overall workspace of the stage, the maximum inscribed rectangular workspace of  $109.4 \times 112.2 \mu\text{m}^2$  can be obtained.

The predicted results match well with the experimental ones, specifically, the relative errors of



(a)



(b)

Fig. 7. Displacement of output platform when (a) maximum input displacement is applied in  $x$ -axis; (b) positioning errors in full range of motion.

experimental results to analytical ones are 6.1% and 3.7%, in  $x$ - and  $y$ -directions, respectively; Whereas the errors of experimental results to FEA ones are 1.9% and 0.75%, correspondingly. In addition, as results of the experiment, the reduction ratio of the precise positioning stage is about 0.313 and 0.321 in  $x$ - and  $y$ -directions, respectively. Table 1 lists the measured results in  $x$ -direction.

Figure 7(b) shows the positioning errors in full range of motion when the stage is positioned in direction of  $x$ -axis, along which maximum input displacement is applied. The errors are  $-0.59 \sim 0.54 \mu\text{m}$ ,  $-0.40 \sim 0.40 \mu\text{m}$  and  $-0.71 \sim 0.69 \mu\text{m}$  in directions of  $x$ -,  $y$ - and  $z$ -axes, respectively.

Table 1  
Measured results in direction of x-axis

axis	Mean ( $\mu\text{m}$ )	Standard deviation ( $\mu\text{m}$ )	SE of mean ( $\mu\text{m}$ )
x	0.00469	0.34561	0.06110
y	-0.01000	0.23762	0.04201
z	-0.02531	0.36055	0.06374
Axis	Min ( $\mu\text{m}$ )	Max ( $\mu\text{m}$ )	Range ( $\mu\text{m}$ )
x	-0.59	0.54	1.13
y	-0.40	0.40	0.80
z	-0.71	0.69	1.40

Table 2  
The measured results in y-direction

Axis	Mean ( $\mu\text{m}$ )	Standard deviation ( $\mu\text{m}$ )	SE of mean ( $\mu\text{m}$ )
y	-0.00125	0.24413	0.04316
x	0.01094	0.28409	0.05022
z	0.01750	0.23772	0.04202
Axis	Min ( $\mu\text{m}$ )	Max ( $\mu\text{m}$ )	Range ( $\mu\text{m}$ )
y	-0.39	0.44	0.83
x	-0.60	0.52	1.12
z	-0.46	0.46	0.92

Table 3  
The results from analytical approach, FEA simulation and experimental study

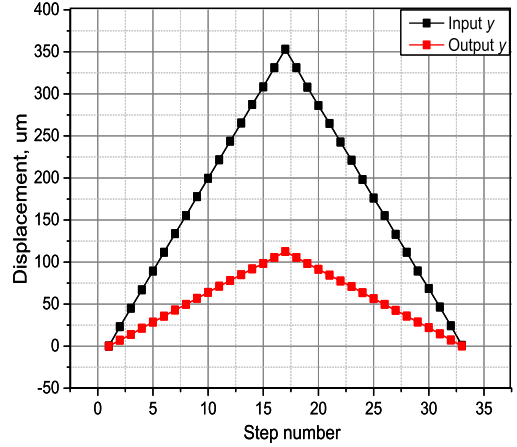
Method	Input data		Average
	Maximum input displacement $\eta_1 = 350 \mu\text{m}$	Minimum input displacement $\eta_1 = 0.5 \mu\text{m}$	
Analytical (x, y)	116.50	0.162	0.3294
FEM, x-axis motion	111.53	0.155	0.3077
FEM, y-axis motion	113.05	0.157	0.3082
Measured, x-axis motion	109.40	0.157	0.3126
Measured, y-axis motion	112.20	0.160	0.3206

When the stage is positioned and applied the maximum input displacement in y-direction, the errors in full range of motion is shown in Fig. 8(b). The errors are  $-0.60 \sim 0.52 \mu\text{m}$ ,  $-0.39 \sim 0.44 \mu\text{m}$ , and  $-0.46 \sim 0.46 \mu\text{m}$  in directions of x-, y- and z-axes, respectively. The measured results in y-direction are listed in Table 2.

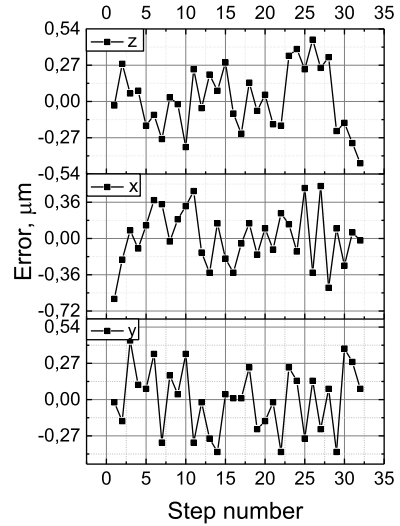
For a clear comparison, the results of the precise positioning stage evaluated by the analytical approach, FEA simulation and experimental study are tabulated in Table 3.

## 7. Conclusions

A new planar precise positioning stage on the rotating platform for calibrating the raster scales



(a)



(b)

Fig. 8. Displacement of output platform when (a) maximum input displacement is applied in y-axis; (b) positioning errors in full range of motion.

of rotary encoder with mechanical actuation is designed and machined. The stage constructed in this study has a rectangular workspace with area of  $109.4 \times 112.2 \mu\text{m}^2$  and positioning resolution of  $0.157 \mu\text{m}$  and  $0.160 \mu\text{m}$  in directions of x- and y-axes, respectively. Its reduction ratios of the input displacement are  $0.313 \mu\text{m}$  and  $0.321 \mu\text{m}$  in the x- and y-directions, correspondingly. The analytical results for the established stage model are well verified by FEA simulation, and validated further by experimental study. The established method can also be applied to model other types of flexure-based precise positioning stage.

## ACKNOWLEDGMENTS

This work was supported by the National Natural Science Foundation of China [Grant No.51475211] and Research Project [Grant No.MIP078/15] funded by the Lithuanian Science Council.

## References

- [1] P. Vasiljev, S. Borodinas, S.J. Yoon and D. Mažeika, The actuator for micro moving of a body in a plane, *Materials Chemistry and Physics* **91**(1) (2005), 237–242.
- [2] J. Dong, Q. Yao and P.M. Ferreira, A novel parallel-kinematics mechanisms for integrated, multi-axis nano positioning. Part 2: Dynamics, control and performance analysis, *Precision Engineering* **32**(1) (2008), 20–33.
- [3] Y. Huang and C. Cheng, Robust tracking control of a piezo-driven monolithic flexure-hinge stage, *Science in China Series G: Physics, Mechanics and Astronomy* **52**(6) (2009), 926–934.
- [4] T. Mohammad and S. Salisbury, Design considerations for long travel Z-axis ultra-precision positioning stage, *International Journal of Precision Engineering and Manufacturing* **13**(9) (2012), 1581–1588.
- [5] Mohd, M.N. Zubir, B. Shirinzadeh and Y. Tian, Development of a novel flexure-based micro-gripper for high precision micro-object manipulation, *Sensors and Actuators A: Physical* **150**(2) (2009), 257–266.
- [6] L. Yangmin and X. Qingsong, Modeling and performance evaluation of a flexure-based XY parallel micro-manipulator, *Mechanism and Machine Theory* **44**(12) (2009), 2127–2152.
- [7] K.B. Choi, J.J. Lee and S. Hata, A piezo-driven compliant stage with double mechanical amplification mechanisms arranged in parallel, *Sensors and Actuators A: Physical* **161**(1–2) (2010), 173–181.
- [8] Y. Li, S. Xiao, L. Xi and Z. Wu, Design, modeling, control and experiment for a 2-DOF compliant micro-motion stage, *International Journal of Precision Engineering and Manufacturing* **15**(4) (2014), 735–744.
- [9] L. Yangmin and X. Qingsong, A novel piezo-actuated XY stage with Parallel, decoupled, and stacked flexure structure for micro/nano-positioning, *IEEE Transactions on Industrial Electronics* **58**(8) (2011), 3601–3615.
- [10] D. Kim, D. Kang, J. Shim, I. Song and D. Gweon, Optimal design of a flexure hinge-based XYZ atomic force microscopy scanner for minimizing Abbe errors, *Review of Scientific Instruments* **76**(073706) (2005), 703–706.
- [11] Q. Xu and Y. Li, Analytical modeling, optimization and testing of a compound bridge-type compliant displacement amplifier, *Mechanism and Machine Theory* **46**(2) (2011), 183–200.
- [12] Q. Yao, J. Dong and P.M. Ferreira, A novel parallel-kinematics mechanisms for integrated, multi-axis nanopositioning. Part 1. Kinematics and design for fabrication, *Precision Engineering* **32**(1) (2008), 7–19.
- [13] J.W. Ryu, S.Q. Lee, D.G. Gweon and K.S. Moon, Inverse kinematic modeling of a coupled exure hinge mechanism, *Mechatronics* **9**(6) (1999), 657–674.
- [14] L. Yangmin and X. Qingsong, Adaptive sliding mode control with perturbation estimation and PID sliding surface for motion tracking of a piezo-driven micro-manipulator, *IEEE Transactions on Control Systems Technology* **18**(4) (2010), 798–810.
- [15] J.H. Kim, Visually guided 3D micro positioning and alignment system, *International Journal of Precision Engineering and Manufacturing* **12**(5) (2001), 797–803.
- [16] S.K. Ro and J.K. Park, A compact ultra-precision air bearing stage with 3-DOF planar motions using electromagnetic motors, *International Journal of Precision Engineering and Manufacturing* **12**(1) (2011), 115–119.
- [17] Y. Tian, B. Shirinzadeh and D. Zhang, Design and dynamics of a 3-DOF flexure-based parallel mechanism for micro/nano manipulation, *Microelectronic Engineering* **87**(2) (2010), 230–241.
- [18] X. Tang and I. Chen, Synthesis and stiffness modeling of XYZ flexure parallel mechanisms with large-motion and decoupled kinematic structure, *Frontiers of Mechanical Engineering in China* **4**(2) (2009), 160–172.
- [19] H. Vahid and T. Tegoeh, Dynamic modeling of 3-DOF pyramidal-shaped piezo-driven mechanism, *Mechanism and Machine Theory* **70** (2013), 225–245.
- [20] T.L. Yung, M.C. Kuo and Z.L. Wen, Model reference adaptive control for a piezo-positioning system, *Precision Engineering* **34**(1) (2010), 62–69.
- [21] S.R. Park and S.H. Yang, A mathematical approach for analyzing ultra precision positioning system with compliant mechanism, *Journal of Materials Processing Technology* **164-165** (2005), 1584–1589.
- [22] D. Zhang, Z. Gao, M. Malosio and G. Coppola, Analysis of the novel flexure parallel micro-manipulators based on multi-level displacement amplifier with/without symmetrical design, *International Journal of Mechanics and Materials in Design* **8**(4) (2012), 311–325.
- [23] H. Wang and X. Zhang, Input coupling analysis and optimal design of a 3-DOF compliant micro-positioning stage, *Mechanism and Machine Theory* **43**(4) (2008), 400–410.
- [24] Q. Xu and Y. Li, Tracking performance characterization and improvement of a piezo-actuated micro-positioning system based on an empirical index, *Robotics and Computer-Integrated Manufacturing* **26**(6) (2010), 744–752.
- [25] E.J. Hwang, K.S. Min, Song, S.H. Ahn, I.H. Choi and W.C., Optimal design of a flexure hinge precision stage with a lever, *Journal of Mechanical Science and Technology* **21**(4) (2007), 616–623.
- [26] Y. Li and Q. Xu, Design and analysis of a totally decoupled flexure-based XY parallel micromanipulator, *IEEE Transactions on Robotics* **25**(3) (2009), 645–657.
- [27] Y. Li and Q. Xu, Development and assessment of a novel decoupled XY parallel micro-positioning platform, *IEEE/ASME Transactions on Mechatronics* **15**(1) (2010), 125–135.
- [28] N. Lobontiu and G. Garcia, Analytical model of displacement amplification and stiffness optimization for a class of flexure-based compliant mechanisms, *Computers and Structures* **81**(32) (2003), 2797–2810.
- [29] D. Mukhopadhyay, J. Dong, E. Pengwang and P. Ferreira, A SOI-MEMS-based 3-DOF planar parallel-kinematics nanopositioning stage, *Sensors and Actuators A: Physical* **147**(1) (2008), 340–351.
- [30] J.H. Kim, S.H. Kim and Y.K. Kwak, Development and optimization of 3-D bridge-type hinge mechanism, *Sensors and Actuators A* **116**(3) (2004), 530–538.
- [31] Y.K. Yong and T.F. Lu, The effect of the accuracies of flexure hinge equations on the output compliances of pla-

nar micro-motion stages, *Mechanism and Machine Theory* **43**(3) (2008), 347–363.

- [32] Y.K. Yong and T.F. Lu, Kinetostatic modeling of 3-RRR compliant micro-motion stages with flexure hinges, *Mechanism and Machine Theory* **44**(6) (2009), 1156–1175.

- [33] J.M. Paros and L. Weisbord, How to design flexure hinge, *Machine Design* **37** (1965), 151–157.